

## THE USE OF SINGLE-CRYSTAL IRON FRAMES IN TRANSIENT FIELD MEASUREMENTS

P. C. ZALM\*, J. VAN DER LAAN and G. VAN MIDDELKOOP

*Fysisch Laboratorium, Rijksuniversiteit Utrecht, P.O. Box 80.000, 3508 TA Utrecht, The Netherlands*

Received 3 January 1979

Single-crystal Fe frames have been investigated for use as a ferromagnetic backing in transient magnetic field experiments. For this purpose the surface magnetization as a function of applied magnetic field has been determined with the magneto-optical Kerr effect. The frames, which have two sides parallel to the  $\langle 100 \rangle$  crystal axis, can be fully magnetized at low external fields such that fringing fields are negligibly small. These single-crystal Fe backings have been used in several transient magnetic field experiments. Comparison of the measured precession angles with previous results, obtained in polycrystalline Fe foils at high external magnetic fields, shows that the single-crystal backings are satisfactory. After extended periods of heavy-ion bombardment the crystals exhibited no radiation damage effects. The absence of fringing fields leads to a reduction of a factor of four in the measuring time for transient field experiments.

### 1. Introduction

The strong transient magnetic field is a powerful tool for measuring magnetic dipole moments of short-lived ( $\tau_m = 0.1$ – $10$  ps) excited nuclear states. In the transient field implantation perturbed angular correlation (TF-IMPAC) method<sup>1,2</sup>) excited and aligned nuclei, produced by a nuclear reaction, recoil into a (fully) magnetized ferromagnetic medium. During the slowing down the nucleus experiences the strong transient magnetic field<sup>3</sup>), which through the interaction with the nuclear magnetic moment causes the spin of the excited state to precess. This precession is observed as a rotation of the angular distribution of the  $\gamma$ -rays emitted in the decay of this state. The measured rotation is an integral over the slowing-down history weighted by the nuclear decay probability. Once the calibration of these dynamic fields as a function of recoil velocity and atomic number of the moving ion is known, the  $g$ -factor of the excited state can be extracted from the observed precession. The field calibration has been discussed elsewhere<sup>3</sup>), at least for ions with atomic number  $Z \lesssim 20$ . In the present paper we focus our attention on experimental procedures only.

In TF-IMPAC experiments the penetration depth of the recoiling ions in the ferromagnetic backing is typically only 1–5  $\mu\text{m}$ . It is therefore of considerable importance to know the surface magnetization of these backings since the transient field is proportional to the degree of magnetization. In most transient field experiments polycrys-

talline Fe target backings have been used. As has been shown<sup>4</sup>) there may be a striking difference between the surface and bulk magnetization at low magnetizing fields. This phenomenon, a distinctive lag in the surface magnetization, is probably due to demagnetizing fields near the surface. For full surface magnetization external fields of the order of 0.1 T are necessary. This inevitably causes a non-negligible fringing field near the target, which has the following effects. Firstly the beam of incoming particles is bent in the fringing field, which turns the reference axis for the  $\gamma$ -ray angular distribution. Secondly, since  $\gamma$ -rays are always detected in coincidence with outgoing reaction particles at an average angle of  $180^\circ$  to the beam direction, the real mean detection angle is different from  $180^\circ$ . This off-axial detection causes a change in the magnetic substate populations of the nuclear state which is also observed as a rotation of the angular correlation<sup>2</sup>). The result of both effects, called the beam-bending effect, is not calculable except for pure Coulomb excitation. It must therefore be measured independently with a non-ferromagnetic backing and subtracted from the total effect in order to obtain the real transient field rotation angle. Since the experimental conditions for the two measurements should be identical, the resulting experimental errors are approximately equal. Hence the total measuring time required for a given error in the net rotation is four times as long as it would be in the absence of the beam-bending effect.

In the present paper we present a method to circumvent these problems by using a single-crystal iron frame as a target backing. Preliminary results

\* Present address: Philips' Natuurkundig Laboratorium, Eindhoven, The Netherlands.

have been reported elsewhere<sup>5</sup>). Integral precession measurements on several nuclei with the single-crystal backing are compared with results obtained with a conventional set-up. It will be shown in the following, through measurements of the magneto-optical Kerr effect<sup>6</sup>), that the surface of single-crystal Fe frames can be magnetized completely at fairly low external fields, for which the corresponding fringing fields are negligibly small.

## 2. Surface magnetization measurements

### 2.1. THE MAGNETO-OPTICAL KERR EFFECT

When a beam of linearly polarized light is incident on a metallic surface the reflected beam will also be linearly polarized in the same direction, if the plane of polarization is either perpendicular or parallel to the plane of incidence (defined by the incoming light beam and the normal of the surface). This is no longer true, however, when the reflecting surface is magnetized<sup>6</sup>). In that case the polarization direction of the reflected beam will, in general, be rotated over an angle proportional to the surface magnetization. Three cases can be distinguished, depending on the orientation of the magnetization relative to the reflecting surface and the plane of incidence<sup>4</sup>): (i) *The polar effect*. The magnetization direction is perpendicular to the surface. Though the polarization rotation is largest in this case it is of no use for our purpose, since it is not the configuration used in TF-IMPAC experiments. (ii) *The transverse effect*. The magnetization direction is parallel to the surface, perpendicular to the plane of incidence. No rotation of the plane of polarization occurs. (iii) *The longitudinal effect*. In this case the magnetization direction is parallel to the surface and in the plane of incidence. The effect attains its maximum at an angle of incidence of  $60^\circ$ . The rotation is proportional to the magnetization and has a maximum value of  $5'$  for fully magnetized iron.

The magneto-optical Kerr effect (MOKE) is particularly suited for surface magnetization studies. It probes the outer layers of atoms in a sample. For a wavelength of e.g.  $0.6 \mu\text{m}$  the average penetration depth of the incident light is 12 nm which corresponds to about 40 atomic layers. Thus, if induction measurements of the bulk magnetization as well as MOKE measurements of the surface indicate saturation, one may readily assume saturation along the whole trajectory of the recoiling ions in the ferromagnetic medium. The maximum Kerr effect is reached at the point of saturation,

whilst magnetic flux measurements must always be corrected for the external field contribution. The main disadvantage of the Kerr technique is that it is virtually impossible to perform absolute measurements because the magnitude of the effect depends sensitively on the presence of non-ferromagnetic oxides at the surface.

The interaction of implanted radioactive nuclei with the static magnetic hyperfine field in the ferromagnetic medium has been used as an alternative to study the surface magnetization<sup>7</sup>). These local fields, however, may not always reflect the total magnetization of the medium, so that this method, apart from being time-consuming, is not considered very reliable.

### 2.2. SET-UP

The experimental set-up used for the MOKE measurements is schematically shown in fig. 1. The light beam from a He-Ne laser passes through a Glan-Tompson prism polariser (polarization direction perpendicular to the plane of the drawing). Subsequently part of the beam is split off by a semi-mirror (SM1) for reference purposes. The main beam is incident on the sample (to be magnetized in longitudinal direction) over a total area of  $1 \text{ mm} \times 2 \text{ mm}$ . The reference beam merges with the reflected main beam through a mirror (M) and a semi-mirror (SM2). Both beams are detected after passing an analyser prism in a photomultiplier (PM) which is protected against local over-radiation by a defocussing lens (L) and a colour filter (F). In order to separate the reference beam and the beam reflected from the sample, the reference and incident beams pass through choppers (C1 and C2) running at different frequencies. The signal from the photomultiplier is fed to two lockin amplifiers (LI1 and LI2) which are tuned to the respective chopper frequencies. These frequencies

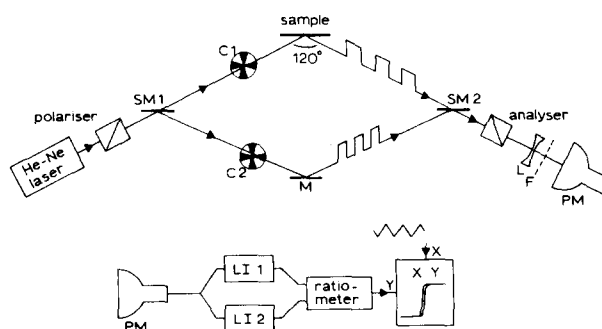


Fig. 1. A schematic representation of the MOKE set-up.

are adjusted such that cross-talk is minimized. Finally the ratio of the output signals of the lock-in amplifiers is fed to the  $y$ -input of an  $x$ - $y$ -recorder. Its  $x$ -input is driven by a signal proportional to the external magnetic field strength applied to the sample.

The laser, the prisms, the semi-mirrors, chopper 1 and the photomultiplier are mounted on two optical benches. The angle between the rails is  $120^\circ$  and the sample holder is placed at the rail intersection. The following steps are involved in the optical alignment:

(i) The sample is mounted with its reflecting surface perpendicular to the beam (angle of incidence of  $\theta = 0^\circ$ ).

(ii) The sample is rotated to the optimum angle of incidence of  $\theta = 60^\circ$  at which the photomultiplier output has a maximum.

(iii) The polariser and analyser are adjusted such that the light incident on the sample is polarized perpendicularly to the plane of incidence and the photomultiplier output has a minimum (polariser and analyser crossed).

(iv) The analyser prism is finally rotated over  $1^\circ$  to generate sufficient light to linearize the photomultiplier output signal as a function of magnetization.

The MOKE set-up is insensitive to intensity variations in the laser beam (as large as 30%) and to changes in sensitivity of the photomultiplier. A typical magnetization curve is shown in fig. 1 in which the direct output of the  $x$ - $y$ -recorder is presented (for details we refer to subsect. 2.3). Small irregularities, probably due to noise in the associated electronics, are observed. Measurements

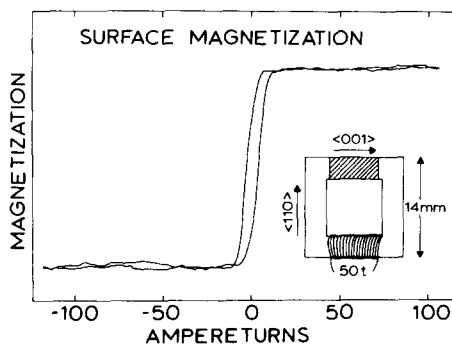


Fig. 2. An example of a hysteresis curve obtained in a MOKE measurement on the  $\langle 001 \rangle$  leg of crystal 1. In the insert the details of the set-up are shown. The laser beam was incident on the hatched area.

on three single-crystal Fe frames and a polycrystalline frame for comparison are discussed below.

### 2.3. RESULTS

The iron window frames which were investigated all have 1 mm thickness, outside dimensions of  $14 \text{ mm} \times 14 \text{ mm}$  and sides of 3 mm wide. Two of the frames are single crystals ( $\alpha$ -Fe, cubic) which were produced at Groningen University. They were made by the strain anneal method<sup>8</sup>), cut by spark erosion and polished and annealed afterwards. The polycrystalline frame was made of armco-iron. Single crystal 1 has two of its sides parallel to within  $30'$  to the  $\langle 001 \rangle$  crystal axis [a direction of easy magnetization; see e.g. ref. 9] and two parallel to the  $\langle 110 \rangle$  axis (see insert in fig. 2). Single crystal 2 has two sides approximately parallel to the  $\langle 100 \rangle$  axis and two approximately to the  $\langle 010 \rangle$  direction. The plane of the frame, however, is at an angle of  $4^\circ$  with the  $\langle 001 \rangle$  crystal plane. Coils of 50 turns around one of the legs were used to magnetize the frames. For such a configuration, one ampere turn corresponds to a magnetizing field of about 24 A/m (80 A/m corresponds to 1 Oe). An example of a MOKE measurement on the  $\langle 001 \rangle$  leg of single crystal 1, is shown in fig. 2. A triangularly varying current with a period of 4 min was applied to the coil. The corresponding magnetizing field changes slowly enough to avoid skin effects. It is interesting to note that the magnetization curve shown in fig. 2 was taken on a spot which had been bombarded with a beam of 35 MeV  $^{12}\text{C}^{5+}$  ions during a period of 150 h at a current of 100 nA.

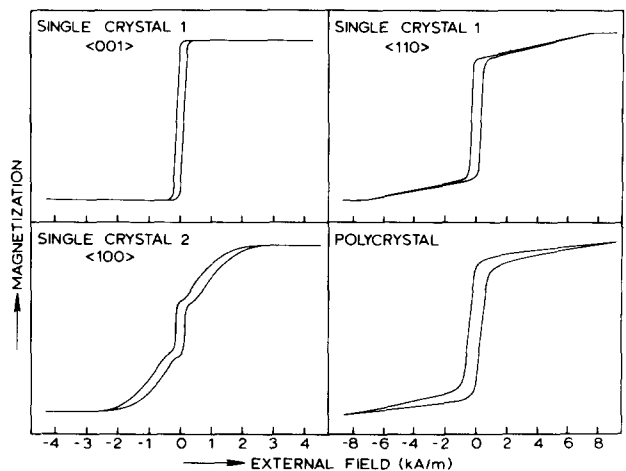


Fig. 3. The results of MOKE measurements on the three iron frames.

The MOKE results for the three window frames are summarized in fig. 3. The curves represent averages over about 10 periods of the external field in order to eliminate the small and unsystematic fluctuations. The magnetization in the  $\langle 001 \rangle$  direction for single crystal 1 shows an almost perfect hysteresis curve. Saturation is reached at 240 A/m. The MOKE curve for the  $\langle 110 \rangle$  direction indicates that 70% of the saturation is reached within 400 A/m but that full saturation is only obtained at about 8 kA/m. For single crystal 2 a peculiar behaviour is found in the surface magnetization. Full saturation is attained at an external field of about 2.5 kA/m. The MOKE measurement on the polycrystalline frame shows that no saturation is obtained even at 8 kA/m, although an appreciable fraction (70%) of the saturation magnetization is reached with an external field of only 1.5 kA/m. This frame was also investigated with fast pulsed magnetizing currents (10 s period) corresponding to fields up to 30 kA/m. These measurements indicate that full saturation is only obtained above 25 kA/m.

From measurements with a small-size Hall probe (diam. 1 mm) near the crystal surface and at a magnetizing field of 3 kA/m, an upper limit for the magnetic induction of 0.2 mT was estimated for the fringing field. This is at least 100 times as small as in the conventional set-up with a large electromagnet<sup>2</sup>). This means that beam-bending effects are negligible indeed. Hence both single crystals may be considered useful as a target backing in TF-IMPAC experiments.

Magnetic induction measurements of the bulk magnetization of the window frames were also performed. For both single crystals the resulting hysteresis curves showed a behaviour very similar to the MOKE curve of the surface in the  $\langle 001 \rangle$  direction of single crystal 1 (upper left corner in fig. 3). For the polycrystalline frame the bulk and surface hysteresis curves showed no significant difference.

Our findings support the tentative conclusion<sup>4</sup>) that the observed lag in the surface magnetization of single-crystal and polycrystalline Fe strips is due to demagnetizing fields owing to the open ends (poles). In closed frames this effect is absent. The distinct lags in the surface magnetization in the  $\langle 110 \rangle$  direction of single crystal 1 and single crystal 2 are of different origin. In these cases the direction of easy magnetization does not coincide with the sides of the frame. This gives rise to

small domains with a magnetization opposite to the field direction ["fir-tree" patterns, see e.g. ref. 9] at low magnetizing fields. Only at higher fields are these domains aligned.

Since (cubic) single-crystal Fe frames are difficult to manufacture, the  $\alpha$ -modification not being the most stable form of crystallization, we have also briefly tested an Fe(Si) single-crystal frame\*. Cubic single crystals are easily grown from Fe with a few (weight) percent of Si mixed in. The magnetization of such Fe(Si) frames, which has been subject to extensive studies<sup>9,10</sup>), shows a behaviour analogous to that of pure iron. Indeed, MOKE measurements of the surface magnetization showed a nice hysteresis curve. Saturation was reached at  $H \approx 1$  kA/m. Since the transient field strength is thought to be proportional to the density of polarized electrons in the ferromagnetic host<sup>3</sup>), the precession effects for a Fe(Si) frame are expected to be equal to within a few percent to those obtained by the conventional method; see subsect. 3.2.

### 3. Application to transient field IMPAC measurements

In this section we describe a number of TF-IMPAC integral precession measurements to test the single crystal frames. The results obtained with these frames are compared with those obtained in the conventional set-up.

#### 3.1. SET-UP AND INTERPRETATION

The "conventional" set-up used in our laboratory for TF-IMPAC integral precession measurements has been described in detail in ref. 2. The associated data collection system, which includes a CDC 1700 on-line computer, has been described in ref. 11. We only mention the details relevant to the present work. Outgoing reaction particles are detected in a 200  $\mu\text{m}$  thick annular Si surface barrier detector, which subtends angles between 166° and 173°. Gamma-radiation coincident with particles is detected in four 12.7 cm diam. by 12.7 cm long NaI(Tl) detectors at angles of  $\pm 72^\circ$  and  $\pm 108^\circ$  to the beam direction in the horizontal plane and at a distance of 20 cm from the target. Targets are evaporated on polycrystalline Fe strips

\* Obtained from Dr. B. Hutchinson, University of Birmingham, U.K.; composition Fe+1.5% (weight) Si. Outside dimensions 17 mm  $\times$  17 mm, sides 4 mm wide and thickness 2 mm. The legs are in the  $\langle 100 \rangle$  and  $\langle 010 \rangle$  crystal directions to within 1°.

with thickness of 5 or 10  $\mu\text{m}$ . These strips are magnetized in a magnetic induction of 0.15 T generated by an electromagnet. The magnetization direction is reversed automatically every 2 min to avoid systematic effects.

For the present measurements an iron frame with the magnetizing coil and the target were placed in the position where formerly the targets on polycrystalline backings were situated in the gap of an electromagnet. Owing to the absence of the return yoke of the electromagnet two additional NaI(Tl) counters were positioned at  $\pm 18^\circ$  to the beam direction to improve statistics. The target material was deposited on the centre part of one of the legs of the frame parallel to the  $\langle 100 \rangle$  or an equivalent direction. This side was then placed vertically in the target chamber such that the incoming beam was perpendicular to the frame to within a few degrees. The heat conduction to the frame support is sufficiently good to avoid excessive heating of the frame by the beam.

Since the outgoing reaction particles are detected in a ring counter (see above) the recoiling ions penetrating the single-crystal Fe lattice have directions between two cones. Therefore only a small fraction of the ions may have a direction fulfilling channeling conditions in the crystal. This may be important since the transient field might be different in a channel. From kinematics one readily estimates, however, that the fraction of channeling ions does not exceed 4% for the reactions investigated.

The integral spin precession angle is deduced from the rotation angle of the  $\gamma$ -ray angular correlation pattern. For this purpose coincident  $\gamma$ -rays were collected at the afore-mentioned detection angles of  $\frac{1}{2}\pi(n \pm \frac{1}{2})$  with  $n = 0, \pm 1$ , which are optimum for correlations of a fully aligned  $2^+$  state<sup>2</sup>). The mean integral precession angle  $\Delta\theta$  can be expressed as

$$\Delta\theta = \frac{\sqrt{r-1}}{\sqrt{r+1}} \cdot \left[ \frac{1}{W(\theta)} \frac{dW(\theta)}{d\theta} \right]^{-1}, \quad (1)$$

where  $W(\theta)$  represents the angular correlation function. The double ratio  $r$  is defined by

$$r = \frac{N[\frac{1}{2}\pi(n+\frac{1}{2})]\uparrow \cdot N[\frac{1}{2}\pi(n-\frac{1}{2})]\downarrow}{N[\frac{1}{2}\pi(n+\frac{1}{2})]\downarrow \cdot N[\frac{1}{2}\pi(n-\frac{1}{2})]\uparrow}, \quad (2)$$

where  $N[\phi]\uparrow\downarrow$  denotes the number of coincident counts accumulated in the  $\gamma$ -ray detector at angle  $\phi$  with magnetic field up or down. For the four  $\gamma$ -

ray detectors at  $\pm 72^\circ$  and  $\pm 108^\circ$  the cross effect  $\varepsilon_c$ , given by

$$\varepsilon_c = \frac{N[\frac{1}{2}\pi(1 \pm \frac{1}{2})]\uparrow \cdot N[-\frac{1}{2}\pi(1 \mp \frac{1}{2})]\downarrow}{N[\frac{1}{2}\pi(1 \pm \frac{1}{2})]\downarrow \cdot N[-\frac{1}{2}\pi(1 \mp \frac{1}{2})]\uparrow} - 1, \quad (3)$$

was used as a check on the measurement. This effect was always found to be zero within the error as it should.

The calibration of the double ratio  $r$  against rotation angle was obtained in the present work by measuring  $\varepsilon$  for a rotation of  $2^\circ$ . This was performed by off-setting the six-counter array by  $\pm 2^\circ$  with the magnetic field set to zero.

### 3.2. RESULTS AND DISCUSSION

Transient field precession measurements were performed on the first-excited  $2^+$  states of  $^{28}\text{Si}$ ,  $^{20}\text{Ne}$ ,  $^{12}\text{C}$  and  $^{18}\text{O}$ . The reasons for selecting these cases are discussed below.

(i) The first-excited state of  $^{28}\text{Si}$  was chosen because it is typical for most low-velocity measurements with light projectiles. This case has also provided the cleanest, fastest and most accurate of all transient field measurements performed with the conventional set-up<sup>12</sup>).

(ii) The case of  $^{20}\text{Ne}$  is typical for a high-velocity measurement with energetic heavy projectiles. Large precessions are expected since the transient field increases with recoil velocity<sup>3</sup>). Since the  $^{20}\text{Ne}$  ions are produced in the heavy-ion  $^{12}\text{C}(^{12}\text{C}, \alpha)$  reaction this case may also provide a good test on possible radiation damage of the single-crystal lattice.

(iii) For the first-excited  $2^+$  state of  $^{12}\text{C}$  a reasonably accurate TF-IMPAC result has been obtained by the Bonn-Strasbourg group<sup>13</sup>) by the conventional method. Because the lifetime of this state is very short,  $\tau_m = 65 \pm 3$  fs [ref. 14], this case tests the single-crystal surface magnetization best. The average probing depth only amounts to 0.4  $\mu\text{m}$ .

(iv) The first-excited state of  $^{18}\text{O}$  has previously been subject to an accurate TF-IMPAC experiment<sup>15</sup>) in this laboratory. Since this state has a lifetime ( $\tau_m = 2.8$  ps) long compared to the stopping time (0.7 ps), this case seemed especially useful as a test of an Fe(Si) frame, since the possible differences of both the (small) static and the dynamic field as compared to those in pure iron can be examined simultaneously.

The details relevant to the experimental condi-

TABLE 1

Summary of the experimental conditions and observed integral precessions for the  $^{28}\text{Si}$ ,  $^{20}\text{Ne}$ ,  $^{12}\text{C}$  and  $^{18}\text{O}$  measurements and a comparison to previous results.

Nucleus ( $E_x$ [MeV]; $\tau_m$ [ps])	Reaction	Beam		Target <sup>a</sup> $d$ [ $\mu\text{g}/\text{cm}^2$ ]	Single crystal <sup>b,c</sup>		Conventional <sup>c</sup>	
		$E$ [MeV],	$I$ [nA]		$t$ [h]	$\Delta\theta$ [mrad]	$t$ [h]	$\Delta\theta$ [mrad]
$^{28}\text{Si}$ (1.78; 0.70)	$^{28}\text{Si}(\alpha, \alpha')$	7.50;	80 (He <sup>+</sup> )	170	30	1.40 ± 0.09	106	1.42 ± 0.15 <sup>d</sup>
			45 (He <sup>+</sup> )		19	1.43 ± 0.15		
$^{20}\text{Ne}$ (1.63; 1.04)	$^{12}\text{C}(^{12}\text{C}, \alpha)$	35.4;	70 (C <sup>5+</sup> )	200	45	4.8 ± 0.8	90	4.4 ± 1.2 <sup>e</sup>
			60 (C <sup>5+</sup> )		30	4.6 ± 1.0		
$^{12}\text{C}$ (4.43; 0.06)	$^{12}\text{C}(\alpha, \alpha')$	10.2;	50 (He <sup>++</sup> )	20	70	0.65 ± 0.13	≈ 340	0.85 ± 0.14 <sup>f</sup>
							≈ 100	0.71 ± 0.25 <sup>f</sup>
$^{18}\text{O}$ (1.98; 2.82)	$^{18}\text{O}(\alpha, \alpha')$	7.37;	60(He <sup>+</sup> )	180 (NiO)	25	-2.6 ± 0.3	≈ 200	-2.7 ± 0.2 <sup>g</sup>

<sup>a</sup> Natural elemental targets were used, except for  $^{18}\text{O}$  (NiO enriched to 93% in  $^{18}\text{O}$ ).

<sup>b</sup> Single crystal 1 was used in all measurements, except for the first  $^{20}\text{Ne}$  measurement (crystal 2) and the  $^{18}\text{O}$  measurement [Fe(Si) frame].

<sup>c</sup> The symbols  $t$  and  $\Delta\theta$  stand for measuring time and precession angle, respectively.

<sup>d</sup> Ref. 12.

<sup>e</sup> Present work.

<sup>f</sup> Ref. 13, corrected for target thickness (see text).

<sup>g</sup> Ref. 15.

tions in these measurements are summarized in table 1. For  $^{28}\text{Si}$  two measurements were performed with single crystal 1. In the first (see also ref. 5) a magnetizing field of 240 A/m was applied, just sufficient for saturation (see fig. 3), whereas in the second 3.2 kA/m was taken. For  $^{20}\text{Ne}$  first a measurement with single crystal 2 as a target backing and subsequently a (shorter) measurement with single crystal 1 were performed, both at a magnetizing field of 3.2 kA/m. In the experiment on  $^{20}\text{Ne}(2_1^+)$  with the conventional set-up the targets were deposited onto 10 mg/cm<sup>2</sup> thick pure Fe and 0.25  $\mu\text{m}$  thick Ag backings for the effect and beam-bending measurements, respectively. For  $^{12}\text{C}$  only one TF-IMPAC measurement was performed with single crystal 1 at a magnetizing field of 3.2 kA/m. For  $^{18}\text{O}$ , finally, the Fe(Si) single-crystal frame was used as a backing, magnetized by a field of 2 kA/m.

It can be inferred from table 1 that the results with the conventional set-up and those obtained with the single-crystal backings agree well. From the  $^{28}\text{Si}$  experiments we conclude that it suffices to apply a magnetizing field which from the MOKE measurements was found to be just sufficient for saturation. Apparently the saturation properties do not deteriorate under beam conditions. The  $^{20}\text{Ne}$  results indicate that the crystals withstand a heavy-ion beam. The data for crystal 2

(first measurement) also imply that even a non-perfect frame (see subject. 2.3 and fig. 3) can be used. As to the comparison for the  $^{12}\text{C}$  data with those from the work of the Bonn-Strasbourg group one must take into account that the latter have been corrected for  $\gamma$ -ray decay in the target. A similar correction applied to the present data would yield  $\Delta\theta = 0.71 \pm 0.14$  mrad in good agreement with the previous results. Hence, from the  $^{12}\text{C}$  data it is clear that indeed the very surface of the single crystal frame is well magnetized. The present result for  $^{18}\text{O}$  in the Fe(Si) backing also agrees well with the precession angle obtained previously with the conventional set-up. The accuracy of the present and previous data is not sufficient to detect the slight difference (5%) in the density of polarized electrons in the Fe(Si) and pure Fe hosts, which might be reflected in the transient field strength.

From the measuring times given in table 1 the time gain which is attained with single-crystal backings is obvious. Part of this gain is due to the increased number of detectors (six instead of four).

Although the results of the TF-IMPAC measurements prove satisfactory it may be worthwhile to consider the possibility of radiation damage in some detail. Such damage will mainly be caused by the incident beam. There may also be a small contribution from the slowing down ions. In any

case most damage occurs at the end of the trajectory of the projectiles or the recoiling ions, i.e. where the nuclear stopping power dominates. This prevents the possible detection of radiation damage after an IMPAC experiment by a MOKE measurement since the penetration depth of the laser light (10 nm) is only a small fraction of the range of the projectiles or ions (1–10  $\mu\text{m}$ ).

The TF-IMPAC integral precession measurements were analysed in some ten consecutive time intervals to detect a possible decrease in the precession angle. This procedure was only meaningful for the Si measurement. For the other measurements unfortunately the errors are quite large so that a change of the precession angle is virtually undetectable. In fig. 4 the time-dependent results for  $^{28}\text{Si}$  are shown. A least-squares fit with an assumed linear time dependence yields a slope of  $+0.02 \pm 0.02$  mrad/h. The data for  $^{12}\text{C}$ ,  $^{18}\text{O}$  and  $^{20}\text{Ne}$  are consistent with no decrease.

It may after all not be so surprising that radiation damage effects are small for the following reasons.

(i) The incident particles are generally stopped far beyond the penetration depth of the ions (except perhaps in heavy-ion reactions) so that the ions do not traverse a damaged region.

(ii) The transient field is proportional to the ion velocity. Therefore most of the rotation takes place at the beginning of the ion trajectory where no damage is expected.

(iii) The concentration of implanted ions is usually rather low. For most cases this is considerably less than one per  $10^6$  Fe atoms integrated over the total exposure time.

(iv) Often the lifetime of the excited state of the recoiling nucleus is less than the stopping time so that there are no contributions from the end of the ion's trajectory.

#### 4. Conclusion and summary

It has been shown in the present paper by two independent tests, measurements of the surface magnetization by the magneto-optical Kerr effect and measurements of the spin precession, that single-crystal iron frames can be used as magnetized backings in transient field experiments. The main feature of these frames is that they can be magnetized at low magnetic fields such that fringing fields are negligible. This leads to a reduction of the measuring time for transient field experiments by a factor of four or conversely makes more accurate  $g$ -factor measurements on short-lived excited nuclear states possible.

It has been found that if the magneto-optical Kerr effect, which has a probing depth of 10 nm for Fe at a wavelength of  $0.6 \mu\text{m}$ , indicates saturation of the magnetization for a certain magnetic field applied to a single crystal that also transient field precession angles, obtained for that crystal at the same field, agree with previously obtained values. Three single-crystal frames have been investigated. Two of these are made of pure Fe, the third contains 1.5% (weight) Si. These crystals are all well suited for transient field measurements. They could be fully magnetized with fields ranging from 250 A/m to 2.5 kA/m (3–30 Oe). During the transient field measurements, extending over periods of up to 70 h in which the crystals were subject to beams of (heavy) ions, no indication of radiation damage has been found.

Although the advantage of using these single-crystal frames for transient field work is obvious, it should be noticed that they are not well suited for experiments with high-energy light incident particles. In that case the background of back-scattered particles from the rather thick frames is prolific. It must also be realised that detection of outgoing particles at forward angles is impossible. For those cases one could use rather thin (a few  $\mu\text{m}$ ) ferromagnetic backings, which can also be magnetized at fairly low fields (10–25 kA/m) as was found in preliminary Kerr measurements; see also ref. 16.

We are grateful to Professor H. de Waard for suggesting the possibility of using single crystals

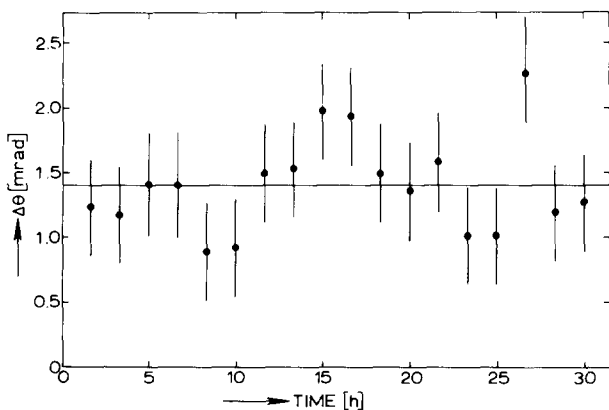


Fig. 4. The measured rotation angle of the angular correlation for the first  $^{28}\text{Si}$  experiment as a function of time. Each point corresponds to a measuring time of 100 min. The line represents the average value.

and for his contributions concerning the Kerr effect measurements. We like to thank Professor A. Wegener Sleswijk and his collaborators at the Laboratory of Metal Physics of the University of Groningen for making the single-crystal pure iron frames. We gratefully acknowledge the help of Miss M. Rots in the surface magnetization measurements and of Drs. J. A. G. De Raedt, R. E. Horstman, W. A. Sterrenburg, Messr. A. Holthuisen and A. J. Rutten during the experiments.

This work was performed as part of the research programme of the "Stichting voor Fundamenteel Onderzoek der Materie" (FOM) with financial support from the "Nederlandse Organisatie voor Zuiver Wetenschappelijk Onderzoek" (ZWO).

## References

- 1) G. K. Hubler, H. W. Kugel and D. E. Murnick, *Phys. Rev. Lett.* **29** (1972) 622 and *Phys. Rev.* **C9** (1974) 1954.
- 2) J. L. Eberhardt, R. E. Horstman, H. W. Heeman and G. van Middelkoop, *Nucl. Phys.* **A229** (1974) 162.
- 3) P. C. Zalm, A. Holthuisen, J. A. G. De Raedt and G. van Middelkoop, *Phys. Lett.* **69B** (1977) 157 and *Hyperfine Interactions* **5** (1978) 347.
- 4) H. de Waard, E. Uggerhøj and G. L. Miller, *J. Appl. Phys.* **46** (1975) 2264.
- 5) P. C. Zalm, J. L. Eberhardt, R. E. Horstman, G. van Middelkoop and H. de Waard, *Phys. Lett.* **60B** (1976) 258.
- 6) J. Kerr, *Philos. Mag.* **3** (1877) 321.
- 7) B. Skaali, R. Kalish and B. Herskind, *Hyperfine Interactions* **1** (1976) 381.
- 8) R. A. Landise, *The growth of single crystals* (Prentice Hall, Englewood Cliffs, N.J., 1971) p. 133.
- 9) S. V. Vonsovskii, *Magnetism*, Vol. 2 (Wiley, New York, 1974).
- 10) H. J. Williams, *Phys. Rev.* **52** (1937) 747; H. J. Williams, R. M. Bozorth and W. Shockley, *Phys. Rev.* **75** (1949) 155; H. J. Williams and W. Shockley, *Phys. Rev.* **75** (1949) 178.
- 11) R. E. Horstman, J. L. Eberhardt, H. A. Doubt, C. M. E. Otten and G. van Middelkoop, *Nucl. Phys.* **A248** (1975) 291.
- 12) J. L. Eberhardt, R. E. Horstman, H. A. Doubt and G. van Middelkoop, *Nucl. Phys.* **A244** (1975) 1.
- 13) M. B. Goldberg, G. J. Kumbartzki, K.-H. Speidel, M. Forterre and J. Gerber, *Hyperfine Interactions* **1** (1976) 429; M. B. Goldberg, E. Konejung, W. Knauer, G. J. Kumbartzki, P. Meyer and K.-H. Speidel, *Phys. Lett.* **58A** (1976) 269.
- 14) F. Ajzenberg-Selove, *Nucl. Phys.* **A248** (1975) 1.
- 15) J. F. A. van Hienen, Ph. D. Thesis (Utrecht, 1975).
- 16) J. C. Adloff, J. Gerber, M. B. Goldberg, W. Knauer, G. J. Kumbartzki and K.-H. Speidel, *Hyperfine Interactions* **4** (1978) 262.